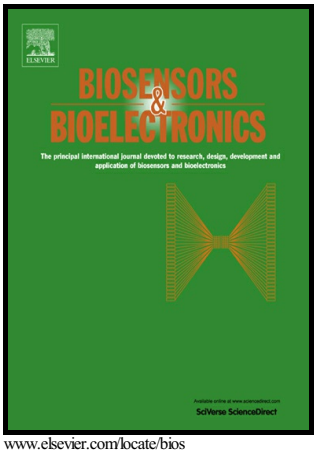

www.elsevier.com/locate/bios

Modified fractal iron oxide magnetic nanostructure: A novel and high performance platform for redox protein immobilization, direct electrochemistry and bioelectrocatalysis application

Hasan Bagheri, Elias Ranjbari, Mohaddeseh Amiri-Aref, Ali Hajian, Yalda Hosseinzadeh Ardakani, Salimeh Amidi

PII: S0956-5663(16)30528-0
DOI: http://dx.doi.org/10.1016/j.bios.2016.05.097
Reference: BIOS8787

To appear in: *Biosensors and Bioelectronic*

Received date: 6 April 2016
Revised date: 18 May 2016
Accepted date: 31 May 2016

Cite this article as: Hasan Bagheri, Elias Ranjbari, Mohaddeseh Amiri-Aref, Al Hajian, Yalda Hosseinzadeh Ardakani and Salimeh Amidi, Modified fractal iror oxide magnetic nanostructure: A novel and high performance platform for redo protein immobilization, direct electrochemistry and bioelectrocatalysi application, *Biosensors and Bioelectronic* http://dx.doi.org/10.1016/j.bios.2016.05.097

Modified fractal iron oxide magnetic nanostructure: A novel and high performance platform for redox protein immobilization, direct electrochemistry and bioelectrocatalysis application

Hasan Bagheri [a,*], Elias Ranjbari [b], Mohaddeseh Amiri-Aref [b], Ali Hajian [c], Yalda Hosseinzadeh Ardakani [b], Salimeh Amidi [d]

[a] *Chemical Injuries Research Center, Baqiyatallah University of Medical Sciences, Tehran, Iran*

[b] *Biopharmaceutics and Pharmacokinetics Division, Department of Pharmaceutics, Faculty of Pharmacy, Tehran University of Medical Sciences, Tehran 14155-6451, Iran*

[c] *Laboratory for Sensors, Department of Microsystems Engineering (IMTEK), University of Freiburg, Georges Köhler Allee 103, 79110 Freiburg, Germany*

[d] *Department of Medicinal Chemistry, School of Pharmacy, Shahid Beheshti University of Medical Sciences, Tehran, Iran*

[*]Corresponding author. Tel.: +98 21824825; fax: +98 21824825

E-mail address: h.bagheri82@gmail.com

Abstract

A novel biosensing platform based on fractal-pattern of iron oxides magnetic nanostructures (FIOMNs) and mixed hemi/ad-micelle of sodium dodecyl sulfate (SDS) was designed for the magnetic immobilization of hemoglobin (Hb) at a screen printed carbon electrode (SPCE). The FIOMNs was successfully synthesized through hydrothermal approach and characterized by atomic force microscopy (AFM), scanning electron microscopy (SEM) and X-ray diffraction

(XRD). In order to provide guidelines for the mixed hemi/ad-micelle formation, zeta-potential isotherms were investigated. The construction steps of the biosensor were evaluated by electrochemical impedance spectroscopy, cyclic voltammetry and Fourier transform infrared spectroscopy. Direct electron transfer of Hb incorporated into the biocomposite film was realized with a pair of quasi-reversible redox peak at the formal potential of -0.355 V *vs.* Ag/AgCl attributing to heme Fe(III)/Fe(II) redox couple. The results suggested that synergistic functions regarding to the hyper-branched and multidirectional structure of FIOMNs and the dual interaction ability of mixed hemi/ad-micelle array of SDS molecules not only induce an effective electron transfer between the Hb and the underlying electrode (high heterogeneous electron transfer rate constant of 2.08 s^{-1}) but also provide powerful and special microenvironment for the adsorption of the redox proteins. Furthermore, the biosensor displayed an excellent performance to the electrocatalytic reduction of H_2O_2 with a detection limit of 0.48 µM and Michaelis-Menten constant (K_m) value of 44.2 µM. The fabricated biosensor represented the features of sensitivity, disposable design, low sample volume, rapid and simple preparation step, and acceptable anti-interferences, which offer great perspectives for the screen-determination of H_2O_2 in real samples.

Keywords: Biosensor; Bioelectrocatalysis; Fractal iron oxides magnetic nanostructure; Mixed hemi/ad-micelle; Protein immobilization; Zeta potential isotherm

1. Introduction

Regarding to the recent development of nanoscience and nanotechnology, a great variety of nanomaterials with interesting morphologies have been used to construct highly sensitive electrochemical sensors and biosensors; such as nanoparticles (Bagheri et al., 2014; Chen et al., 2013), nanodiamonds (Gopalan et al., 2013), nanotubes (Afkhami et al., 2012; Ji et al., 2015), nanoflowers (Zhu et al., 2011), nanospheres (Rong et al., 2016), and nanosheets (Teymourian et al., 2014; Wu et al., 2012).

It is well-known that nanomaterials can provide a favorable microenvironment for redox proteins and enzymes to realize direct electrochemistry and fabricate excellent third-generation biosensors (Ilkhani et al., 2015; Liu et al., 2009) as well as biofuel cells (Liu et al., 2013). In addition, it is proved that the modification of the electrode surface with nanomaterials accelerates the direct electron transfer between electrodes and redox-active protein (Wang et al., 2013), as the redox proteins show a slow rate of electron transfer on a conventional electrode due to the inaccessibility of the electroactive prosthetic group, the adsorptive denaturation and the unfavorable conformation upon the adsorption on the electrode surface (Liu et al., 2015). Therefore, optimization of the electron transfer between the redox sites of proteins and the electrode surface is certainly desirable. Hence, it is valuable to find ideal electrode materials and suitable protein immobilization techniques.

Fractal structures are common in nature across all length scales, from self-assembled molecules, to the shapes of coastlines, to the distribution of galaxies, and even to the 3D shapes of clouds (Cao et al., 2005). On the nanoscale, dendritic fractals are one type of hyper-branched structures which are generally formed by the hierarchical self-assembly under non-equilibrium conditions (Meakin, 1983). Investigation of hierarchically self-assembled fractal patterns in chemical systems has shown that the distinct size, shape, and chemical functionality of such

structures make them promising candidates for the design and fabrication of new functional nanomaterials (Cao et al., 2005). On the other hand, iron oxide magnetic nanoparticles have been the subject of increasing interest due to their high biocompatibility, super-paramagnetic property, as well as better interaction with biomolecules (Yang et al., 2014). As an ideal biomolecular immobilizing carrier, magnetic nanomaterials offer quick and efficient isolation or extraction of a target biomolecule by an external magnetic field (Jang and Lim, 2010).

Surface modification of nanomaterials, not only are important for engineering their surface energy and interfacial properties, but also for providing active surfaces to attach designated molecules that are immobilized on the surfaces of the nanostructures (Lyon et al., 2004; Putzbach and Ronkainen, 2013). In order to surface modification of as-synthesized FIOMNs, surfactant molecules as physical promoter were applied. Regarding to the biocompatible characteristics of the surfactants, they can provide a good microenvironment to retain the activities of the immobilized proteins (Li et al., 2002). Recently, Amiri-Aref, et al. reported self-assembly of mixed hemimicelles/admicelles (MHAM) of a positively charged surfactant (CTAB) to modify the surface of the magnetic nanoparticles (MNPs) for hemoglobin (Hb) entrapment (Amiri-Aref, et al., 2015). In this work, for the first time, we presented utilization of iron oxide magnetic nanostructures with fractal pattern (so-called fractal iron oxide magnetic nanostructures, FIOMNs) coated by the MHAM arrays of a negatively charged surfactant (SDS) as a novel host for Hb immobilization. The advantage of the present work respect to previous work (Amiri-Aref, et al., 2015) is using the hyper-branched and multidirectional structures of FIOMNs which leads to more efficient entrapment of protein as well as improving the accessibility to the redox prosthetic group of protein. The FIOMNs were successfully synthesized by hydrothermal method and formation of the coating shell was

precisely controlled by zeta potential (Z_P) measurement. To the best of our knowledge, Z_P isotherm for surfactant coated FIOMNs has not yet been reported; although, Z_P data for SDS coating of MNPs was reported, previously (Ranjbari et al., 2015). MHAM is an intermediate zone in Z_P isotherm between hemimicelle and admicelle zone which is providing a dual mechanism for adsorption of amphiphilic targets (Merino et al., 2003). The major advantage of MHAM zone respect to the two other mentioned zones is the ability of MHAM in establishing of both electrostatic and hydrophobic interactions with desired biomolecules. Therefore, the MHAM array of SDS (MHAMS) coated FIOMNs (MHAMS@FIOMNs) was prepared to Hb entrapment. Owing to the special structure of the FIOMNs, the needed amounts of surfactant to achieve MHAMS coating layer is lower than the ones needed for MNPs reported by Ranjbari et al (Ranjbari et al., 2015) and Du et al (Du et al., 2016). Afterward, the Hb immobilized at the MHAMS@FIOMNs (Hb-MHAMS@FIOMNs) was magnetically captured onto a screen-printed carbon electrode (SPCE) by applying a super magnet underneath the electrode. Finally, at the suggested setup (Hb-MHAMS@FIOMNs/SPCE), the direct electrochemistry of Hb as well as the accurate and sensitive electrocatalytic determination of hydrogen peroxide in an ultra-low sample volume (typically a drop of 50 µL of sample) was successfully achieved. This protein immobilization technique is simple, low cost and effectual, neither the complicated pretreatment steps, nor the particular immobilizing reagent are needed and could be exploited for the fabrication of novel biosensors and bioelectronic devices.

2. Experimental

2.1. Reagents and Instrumentation

The reagents and instrumentation are described in detail in the supplementary information.

2.2. Procedures of the FIOMNs synthesis, MHAMS@FIOMNs preparation and biosensor fabrication

FIOMNs were synthesized according to the procedure which was explained by Sun et al. (Sun et al., 2011). In this procedure α-Fe_2O_3 was synthesized by hydrothermal method according to the method of Cao et al. (Cao et al., 2005) and then dendritic like hierarchical structure of Fe_3O_4 was achieved with the phase transformation of dendritic α-Fe_2O_3 to Fe_3O_4 through the partial reduction. The details of synthesis steps and the size distribution (Fig. S1) of the branches of FIOMNs' trunks are presented in the supplementary information.

Generally, surface modification can be accomplished by physical or chemical adsorption of the desired molecules to coat the surface, depending on the specific applications. Since the synthesized FIOMNs have positive surface charge (Z_P = +33.1 mV) at pH 5.0, the anionic surfactants (here: SDS) can be electrostatically self-assembled at their surfaces. To achieve MHAMS coating shell on FIOMNs, the ratio of SDS to FIOMNs concentration is critical and it was investigated by Z_P measurements. To form the MHAMS@FIOMNs suspension, SDS and FIOMNs were mixed for 5 min using a shaker with the desired concentration ratio ([SDS]/[FIOMNs] = 0.87, section 3.2).

For biosensor fabrication, 20 μL of the MHAMS@FIOMNs suspension (5 mg/mL) were added in 20 μL PBS (pH 5.5) containing Hb (5 mg/mL). The above mixture was stirred gently for 5 min. During the mixing, the Hb molecules were adsorbed on the surface of MHAM@FIOMNs composite (denoted as Hb-MHAMS@FIOMNs). The details of the

optimization of the parameters affecting on the immobilization condition including amount of Hb and amount of MHAMS@FIOMNs were described in supplementary information (Fig. S2). Since its isoelectric point is at about 7.1, Hb is positively charged at pH 5.5 and could be electrostatically adsorbed on the negatively charged nanocomposite surfaces. Besides, the hydrophobic parts of Hb molecules were involved in hydrophobic chains of the surfactants in the MHAMS array. Then, the Hb-MHAMS@FIOMNs biocomposite was isolated from the suspension by placing an Nd-Fe-B super-magnet (1.3 Tesla) at the bottom side of the mixing vial. Afterward, the supernatant solution was taken out and the accumulated Hb-MHAMS@FIOMNs (10 μL) were pipetted onto the surface of screen-printed working electrode. The Hb-MHAMS@FIOMNs biocomposite is captured at SPCE by applying super magnet underneath the working electrode surface. This set-up allows Hb-MHAMS@FIOMNs to be kept on the working electrode surface by avoiding the use of any complex immobilization step, making the whole procedure carried out within a few minutes. The final biosensor is denoted as Hb-MHAMS@FIOMNs/SPCE.

3. Results and discussion

3.1. Characterization of FIOMNs by SEM, AFM and XRD

The morphologies and size distribution of the as-synthesized FIOMNs were characterized using SEM. As it was indicated in Fig. 1A, almost the whole product consist well-defined dendritic fractal structure (a hierarchical structure with a primary trunk consisting of highly disciplined branches distributed on both sides of the trunk). The lengths of the dendrite trunks are 1-3 μm, and those of the branches of trunk range from 50 to 500 nm. Moreover, the surface roughness and three-dimensional (3D) morphology of the FIOMNs were also characterized by

AFM. The results show that the surface roughness of the FIOMNs is below the 50 nm (scan size: 10 μm × 10 μm) (Fig. 1E). Additionally, the structure of the synthesized FIOMNs was characterized by XRD (Fig. 1D). The observed pattern of diffraction peaks is contributed to the planes of (2 2 0), (3 1 1), (4 0 0), (4 2 2), (5 1 1), and (4 4 0) in the crystal structure, which are in accord with characteristic XRD peaks of magnetite (Fe_3O_4) structure according to the Joint Committee on Powder Diffraction Standards (JCPDS No. 19-629).

SEM was also used to characterize and compare the surface morphologies of bare SPCE (Fig. 1B), MHAMS@FIOMNs/SPCE (Fig. 1C) and Hb-MHAMS@FIOMNs/SPCE (Fig. 1D). The figure shows changes in surface morphology of SPCE electrode after its modification by MHAMS@FIOMNs composite and then immobilization of Hb on its surface to fabricate Hb-MHAMS@FIOMNs/SPCE biosensor. The bare SPCE electrode appears the flake graphite surface (Fig. 1B), whereas the surface of MHAMS@FIOMNs/SPCE showed the hyper-branched structure of the MHAMS@FIOMNs (Fig. 1C). The SEM image of Hb-MHAMS@FIOMNs/SPCE (Fig. 1D) obviously showed a globular structural morphology of Hb distribute onto the hyper-branched and multidirectional structures of MHAMS@FIOMNs, indicating the successful immobilization of Hb onto the surface of MHAMS@FIOMNs composite.

Figure 1

3.2. Z_p isotherm studies

Knowledge of the adsorption isotherms of surfactants on the surface of mineral oxides is essential to know the regions where different self-assemblies form (Zhao et al., 2011). The Z_P isotherm is a useful tool for understanding the surface-charge characteristics of the particles

(Zhao et al., 2011) and can be used for exploring the different self-assemblies of surfactants around metal oxides. Normally, ionic surfactant adsorption isotherm on metal oxides is including three regions: hemi-micelles, MHAM, and ad-micelles) (Atkin et al., 2003). Figure 2A indicates the Z_P of FIOMNs' surface versus the different ratios of [SDS] □ [FIOMNs]. Owing to the positive charge of the FIOMNs in acidic conditions (pH = 5.0), the Z_P measurement of bare FIOMNs depicted the value of 33.1 mV. By enhancing the ratio of [SDS] □ [FIOMNs] up to 0.15, the surface charge of FIOMNs was changed from positive values to zero; it means that all the FIOMNs were covered by a monolayer of SDS molecules which it is called hemi-micelle. The formation of this monolayer of SDS molecular array on the surface of FIOMN enables it to make the hydrophobic interaction with Hb molecules. The more concentration of SDS molecules was resulted in the formation of the second layer around the FIOMNs through hydrophobic interaction of their carbon chain; so that the Z_P values changed to minus values due to the negative charge of the SDS molecules in the second layer. As it can be seen in Fig. 2A, the diminution of the slope of Z_P depression is in an exponential manner, insofar as a plateau is formed in [SDS] □ [FIOMNs] ratio of about 1.45; this can be explained by the fact that the enhancement of SDS on the surface of FIOMNs, decreases the tendency of FIOMNs for adsorption of more SDS, sterically and electrostatically. All the FIOMNs are covered by bilayer of SDS molecules at the [SDS] □ [FIOMNs] ratio of 1.45; this bilayer molecular array of SDS molecules is called ad-micelle and enables FIOMNs to possess only the electrostatic interaction with Hb molecules. At the ratios more than 1.45, despite increasing the SDS concentration, the Z_P was fixed; because there wasn't any empty place on the surface of FIOMNs and the concentration of SDS was increased just in the aqueous solution. Between the [SDS] □ [FIOMNs] ratios of 0.15 and 1.45, some parts of each FIOMNs are coated as bilayer and the

other parts remain as monolayer; this self-assembly array of SDS molecules around FIOMNs is called mixed hemi/ad-micelle (MHAMS) and lets the FIOMNs to have both hydrophobic and electrostatic interactions with Hb molecules. The MHAMS not only protects the FIOMNs chemically and physically, but also this kind of SDS molecular array provides a substrate around the FIOMNs, which is able to attract positively charged amino acid residues of Hb (pH 5.5) electrostatically through their negatively charged head groups as well as making hydrophobic interaction with hydrophobic regions of the Hb molecule through their hydrophobic tails (Fig. 2B); thus, the subsequent experiments were performed using the MHAMS@FIOMNs.

The optimum ratio of [SDS]/[FIOMNs] in the MHAMS zone for Hb immobilization was determined through cyclic voltammetry (CV) experiments. Based on the obtained data (Table S1), the ratio of 0.87 was selected as an optimum point for hemoglobin entrapment. Moreover, the Z_P value of -23.6 mV in the selected ratio indicates the stability of MHAMS@FIOMNs suspension.

Figure 2

3.3. FT-IR, electrochemical impedance spectroscopy (EIS) and CV characterization

The spectral feature of MHAMS@FIOMNs (a), Hb (b) and Hb-MHAMS@FIOMNs (c) were well illustrated in supporting information (Fig. S3). The results of FT-IR spectroscopy suggested the successful immobilization of Hb on the surface of MHAMS@FIOMNs.

EIS has proved to be one of the most powerful tools for interfacial investigations to demonstrate the successful immobilization of molecules (e.g. redox proteins) onto the electrode surface during preparation of a biosensor (George and Lee, 2009; Shi et al., 2007). The electron transfer resistance (R_{ct}) can be used to describe the interfacial properties of the electrode which

correspond to the electron-transfer kinetics of the redox probe and can be estimated from the diameter of the semicircle domain at a higher frequency of the impedance spectra. Figure 3 illustrates Nyquist plots of the electrode surface at different preparation steps in 0.1 M KCl solution containing 10 mM of the redox probe $K_3[Fe(CN)_6]/K_4[Fe(CN)_6]$. As can be seen, significant changes in the impedance results were observed during the stepwise modification process. From the Randel's equivalence circuit model (Fig. 3, inset), the double layer capacitance (C_{dl}), Warburg impedance (W), electrolyte resistance (R_s) and R_{ct} values were calculated (Table S2). On the bare SPCE, the R_{ct} value was estimated as 106 Ω (curve a). After dripping MHAM@FIOMNs/SPCE on the surface of the electrode a semicircle of about 217 Ω was observed (curve b), while the assembly of Hb at the surface of MHAM@FIOMNs/SPCE was resulted in the obvious increment of the electron transfer resistance (R_{ct} of 661 Ω, curve c), due to the non-conductive nature of the protein molecules which hindered the electron transfer of the redox probe. However, the obtained R_{ct} for Hb-MHAM@FIOMNs/SPCE was highly decreased in comparison with Hb-SPCE (R_{ct} of 2372 Ω, Fig. S4). The EIS data are in good agreement with the CV behaviors as shown in Fig. 3B. The obtained results clearly imply that the Hb was immobilized onto the surface of the MHAMS@FIOMNs nanocomposite.

Figure 3

3.4. Direct electrochemistry of Hb-MHAMS@FIOMNs/SPCE

Immobilization of Hb onto MHAM@FIOMNs nanocomposite was further investigated by recording cyclic voltammograms of bare SPCE, Hb/SPCE, Hb-MHAMS/SPCE and Hb-MHAMS@FIOMNs/SPCE in 0.1 M pH 7.0 PBS at a scan rate of 100 mVs^{-1} in deaerated medium (Fig. 4A). On bare SPCE (curve a) and Hb/SPCE (curve b) no electrochemical signal appeared, indicating that no redox substances were present on the electrode surface. At the

surface of Hb-MHAMS/SPEC, a pair of small redox peak appeared (curve c), which is indicated that mixed hemi/ad-micelle array of SDS can promote the direct electron transfer of Hb to some extent. However, at Hb-MHAMS@FIOMNs/SPCE a couple of well-defined redox peaks were clearly observed (curve d). The obtained results can be attributed to the presence of the fractal iron oxide magnetic nanostructures in the composite film, which is biocompatible with a specific high surface area that can improve the accessibility to the Hb, resulted in the favorable microenvironment for the protein entrapment. In fact, a synergistic function regarding to the integration of the advantages of the fractal iron oxide magnetic nanostructures (the hyper-branched and multidirectional structures of FIOMNs) and the mixed hemi/ad-micelle array of SDS molecules (two-folds interactions with protein-either electrostatic or hydrophobic) led to effective electrons shuttle between protein molecule and the underlying electrode, so the direct electron transfer of Hb was realized at the Hb-MHAMS@FIOMNs/SPCE. As it can be seen in Fig. 4A (curve c), the values of cathodic peak potential (E_{pc}) and anodic one (E_{pa}) at Hb-MHAMS@FIOMNs/SPCE were obtained as −0.41 and −0.30 V which is in accordance with the characteristic potential of Fe(III)/Fe(II) redox couples of heme proteins. The formal potential ($E^{\circ\prime}$), which is calculated from the average of the redox peak potentials, was estimated to be −0.355 V vs. Ag/AgCl. Peak-to-peak separation (ΔEp) was obtained as 0.110 V and the ratio of cathodic peak current over the anodic one is nearly unit. Therefore, based on these electrochemical parameters, the direct electron transfer of Hb in MHAMS@FIOMNs film is considered as a quasi-reversible process. Figure 4B displays a schematic diagram of the Hb-MHAMS@FIOMNs/SPCE biosensor set-up for magnetic immobilization of Hb at SPCE.

3.5. Effect of potential scan rate

To further evaluate the characteristics of Hb-MHAMS@FIOMNs/SPCE, the influence of potential scan rate was studied. Figure 4C-a, depicts the cyclic voltammograms of the Hb-MHAMS@FIOMNs/SPCE in 0.1 M PBS (pH 7.0) at different scan rates. The reduction and oxidation peak currents (I_p) exhibit a linear relationship with the scan rate (Fig. 4C-b), indicating a typical surface-controlled electrochemical process. Furthermore, plots of logarithm of the peak currents versus the logarithm of the potential scan rate were linear and had the slopes of about 1 (Fig. 4C-c), which is very close to the expected theoretical slope of 1 for thin-layer voltammetry (Bard and Faulkner, 1980). This result suggests that in this process, all of the electroactive Hb Fe (III), produced by the oxidation of Hb Fe (II) on the anodic scan, could be reduced to Hb Fe (II) on the reverse cathodic scan.

Figure 4

The surface concentration of electroactive species (Γ mol cm^{-2}) can be approximately calculated from the slope of peak currents vs. scan rate. For a reversible surface reaction, the peak current has been given by Eq. (1) (Laviron, 1979a):

$$I_p = \frac{n^2 F^2 A \Gamma \upsilon}{4RT} \quad (1)$$

where A is the geometrical surface area of the electrode, n is the number of electrons transferred, υ is the potential scan rate and F is the Faraday constant. From the slope of cathodic peak currents vs. scan rate, the calculated surface concentration of Hb was estimated to be 3.10×10^{-10} mol cm^{-2}, which is larger than the theoretical monolayer coverage (1.89×10^{-11} mol cm^{-2}) (Wang et al., 2005). The bigger surface concentration can be ascribed to the expanded interspace to hold more Hb molecules, indicating that intercalated Hb in the nanocomposited film participated efficiently in the electron transfer process. Therefore, the MHAMS@FIOMNs is a

promising platform for increasing the functional density of Hb, allowing the electric communication with the underlying SPCE.

By plotting the variation of the peak potential versus the logarithm of the scan rate (Fig.4C-d), the apparent heterogeneous electron transfer rate constant (k_s) and the transfer coefficient (α) for Hb-MHAMS@FIOMNs/SPCE can be calculated based on Laviron's equation (Eq. (2)), derived for a diffusionless process (Laviron, 1979b):

$$E_{pc} = E^{\circ'} - \left[\frac{2.3RT}{\alpha nF}\right]\log\left\{\left[\frac{\alpha nF}{RT}\right]\times\left[\frac{\upsilon}{K_s}\right]\right\} \quad (2)$$

where

$$Slope = -\frac{2.3RT}{\alpha nF} = S \quad (3)$$

$$Intercepte = E^{\circ'} + S\log\left(\frac{-2.3}{S}\right) - S\log\left(K_s\right) \quad (4)$$

According to Eq (3), the transfer coefficient (α) was estimated to be 0.54. The heterogeneous electron transfer rate constant (k_s) was further obtained from Eqs. (3) and (4), and found to be 2.08 s^{-1}, which is superior to those obtained for Hb immobilized in hybrid modified electrodes composed of graphene and multi-walled carbon nanotubes of 0.97 s^{-1} (Sun et al., 2013) and Hb immobilized polyelectrolyte-surfactant polymer and carbon nanotubes of 0.4 s^{-1} (Chen and Lu, 2007), suggesting reasonably fast electron transfer of Hb at the MHAMS@FIOMNs/SPCE.

3.6. Bioelectrocatalytic performance of Hb-MHAMS@FIOMNs/SPCE

Immobilized heme protein on an electrode surface with retained its biological properties normally represents electrocatalytic activity towards H_2O_2 (Dai et al., 2004). Fig. S5 shows the bioelectrocatalytic activity of the Hb-MHAMS@FIOMNs/SPCE biosensor toward the reduction

of H_2O_2 using CV. Since hydrodynamic amperometry is more sensitive than CV, it was employed to estimate the detection limit of H_2O_2 determination. Figure 5A showed a typical steady-state amperometric response of the proposed biosensor with the successive additions of H_2O_2 to pH 7.0 PBS under stirring condition at the applied potential of −0.43 V vs Ag/AgCl. The current response and the concentration of H_2O_2 showed a good linear relationship in the concentration range from 2.0 to 320.0 μM with a correlation coefficient of 0.9838 (Fig. 5B). The detection limit was calculated to be 0.48 μM (S/N=3) which is comparable to the other reported Hb modified electrode (Table S3), demonstrating excellent bioelectrocatalytic activity of Hb immobilized in MHAMS@FIOMNs/SPCE toward H_2O_2 reduction. When the concentration of H_2O_2 became higher than 320.0 μM, the calibration curve reached a plateau and level off, due to the progressive enzyme inactivation in the presence of higher concentrations of H_2O_2 which imply a characteristic behaviour of the Michaelis–Menten kinetic mechanism (Fig. 5C). The apparent Michaelis–Menten constant (K_m), which gives an indication of the enzyme–substrate kinetics, can be calculated according to Lineweaver–Burk equation (Li et al., 1996):

$$\frac{1}{I_{ss}} = \frac{1}{I_{\max}} + \frac{K_m}{I_{\max} C} \quad (5)$$

Where, I_{ss} is the steady-state current after the addition of the substrate, C is the bulk concentration of the substrate and I_{max} is the maximum current measured under saturated substrate solution. K_m can be obtained by the analysis of the slope and the intercept of the plot of the reciprocals of the steady-state current versus H_2O_2 concentration. The K_m value of the system was found to be 44.2 μM which is comparable to those of other Hb-based biosensor (Table S3). As it is well known the smaller K_m shows the higher catalytic ability. The low K_m value suggests that entrapped Hb in MHAMS@FIOMNs composite keeps its biocatalytic activity and exhibits

high affinity toward H_2O_2 reduction. The selectivity (Table S4), reproducibility and stability properties of the developed biosensor are also key factors for its performance, which was explained in the supplementary information.

Figure 5

3.7. Real sample analysis

The applicability and reliability of the proposed biosensor in real samples analysis with different matrices were examined to confirm the usefulness of Hb-MHAMS@FIOMNs/SPCE. The commercial mouthwash, rain water, human urine and serum samples were spiked with different values of H_2O_2 and the measurements were performed using the standard addition method. Satisfactory recovery and RSD values of the experimental results (Table 1) indicate the potential practical applications of the developed biosensor for H_2O_2 determination in real samples.

Table 1

4. Conclusions

The present work describes a novel biosensing platform based on direct electron transfer of hemoglobin immobilized onto nanocomposite containing fractal-like pattern of iron oxides magnetic nanostructures and mixed hemi/ad-micelle configuration of SDS magnetically attached to the screen printed electrode (Hb-MHAMSS@FIOMNs/SPCE). The results demonstrated that the suggested composite matrix could provide a suitable microenvironment for the heme proteins to retain their initial structure and bioactivity, and thus significantly promoted the direct electron transfer between the heme redox center and the underlying electrode. The designed biosensor

exhibited excellent performances for bioelectrocatalytic reduction of H_2O_2 such as high sensitivity, low detection limit, long-term stability and reproducibility. The proposed magnetic entrapment strategy simplifies the redox proteins immobilization associated with the advantages of large adsorption capacity, short immobilization time and no need of complicated covalently attachment or time consuming intermediate step, which can be promising for third generation biosensor and bioelectronics devices fabrication.

Acknowledgements

The authors gratefully acknowledge the support of work by the Research Council Baqiyatallah University of Medical Sciences.

References

Afkhami, A., Bagheri, H., Khoshsafar, H., Saber-Tehrani, M., Tabatabaee, M., Shirzadmehr, A., 2012. Anal. Chim. acta 746, 98-106.

Amiri-Aref, M., Raoof, J.B., Kiekens, F., De Wael, K., 2015. Biosens. Bioelectron. 74, 518–525.

Bagheri, H., Afkhami, A., Panahi, Y., Khoshsafar, H., Shirzadmehr, A., 2014. Mater. Sci. Eng. C, 37, 264–270.

Bard, A.J., Faulkner, L.R., 1980. Electrochemical Methods: Fundamentals and Applications, Wiley, New York.

Cao, M., Liu, T., Gao, S., Sun, G., Wu, X., Hu, C., Wang, Z.L., 2005. Angew. Chem. Int. Edit., 44, 4197–4201.

Chen, L., Lu, G., 2007. Sens. Actuators B 121, 423-429.

Chen, S., Yuan, R., Chai, Y., Hu, F., 2013. Microchim. Acta 180, 15-32.

Dai, Z.H., Liu, S.Q., Ju, H.X., Chen, H.Y., 2004. Biosens Bioelectron. 19, 861–867.

Du, J., Wu, H., An, Y., Shi, Y., Guo, X., Du, L., 2016. Anal. Methods 8, 2778-2785.

George, S., Lee, H.K., 2009. J. Phys. Chem. C 113, 15445–15454.

Gopalan, A.I., Komathi, S., Anand, G.S., Lee, K.P., 2013. Biosens. Bioelectron. *46*, 136–141.

Ilkhani, H., Sarparast, M., Noori, A., Bathaie, S. Z., Mousavi, M. F., 2015. Biosens. Bioelectron. 74, 491-497.

Jang, J. H., Lim, H. B., 2010. Microchem. J. 94, 148–158.

Ji, J., Zhou, Z., Zhao, X., Sun, J., Sun, X., 2015. Biosens. Bioelectron. 66, 590-595.

Laviron, E., 1979a. J. Electroanal. Chem 100, 263–270.

Laviron, E., 1979b. J. Electroanal. Chem. 101, 19–28.

Li, J., Tan, S.N., Ge, H., 1996. Anal. Chim. Acta 335, 137–145.

Li, M., Xu, M., Li, N., Gu, Z., Zhou, X., 2002. J. Phys. Chem. B 106, 4197–4202.

Liu, H., Duan, C., Yang, C., Chen, X., Shen, W., Zhu, Z., 2015. Mater. Sci. Eng. C 53, 43-49.

Liu, J., Guo, C., Li, C. M., Li, Y., Chi, Q., Huang, X., Liao, L. Yu, T., 2009. Electrochem. Commun. 11, 202–205.

Liu, Y., Du, Y., Li, C. M., 2013. Electroanal. 25, 815–831.

Lyon, J. L., Fleming, D. A., Stone, M. B., Schiffer, P., Williams, M. E., 2004. Nano Letters, 4, 719–723.

Meakin, P., 1983. Phys. Rev. Lett., 51, 1119.

Merino, F., Rubio, S., Perez-Bendito, D., 2003. Anal. Chem. 75, 6799–6806.

Putzbach, W., Ronkainen, N. J., 2013. Sensors, 13, 4811-4840.

Ranjbari, E., Hadjmohammadi, M. R., Kiekens, F., De Wael, K., 2015. Anal. Chem., 87, 7894–7901.

Rong, Q., Feng, F., Ma, Z., 2016. Biosens. Bioelectron. 75, 148-154.

Shi, G., Sun, Z., Liu, M., Zhang, L., Liu, Y., Qu, Y., Jin, L., 2007. Anal. Chem. 79, 3581-3588.

Sun, G., Dong, B., Cao, M., Wei, B., Hu, C., 2011. Chem. Mater., 23, 1587-1593.

Sun, W., Cao, L., Deng, Y., Gong, S., Shi, F., Li, G., Sun, Z., 2013. Anal. Chim. Acta 781, 41-47.

Teymourian, H., Salimi, A., Firoozi, S., Korani, A., Soltanian, S. 2014. Electrochim. Acta 143, 196-206.

Wang, J., Zhao, W. W., Zhou, H., Xu, J. J., Chen, H. Y., 2013. Biosens. Bioelectron. 41, 615-620.

Wang, S.F., Chen, T., Zhang, Z.L., Shen, X.C., Lu, Z.X., Pang, D.W., Wong, K.Y., 2005. Langmuir 21, 9260–9266.

Wu, S., Zeng, Z., He, Q., Wang, Z., Wang, S. J., Du, Y., Yin, Z., Sun, X., Chen, W., Zhang, H., 2012. Small 8, 2264-2270.

Yang, Z., Zhang, C., Zhang, J., Bai, W., 2014. Biosens. Bioelectron. 51, 268–273.

Zhu, Z., Li, X., Zeng, Y., Sun, W., Zhu, W., Huang, X., 2011. J. Phys. Chem. C, 115, 12547–12553.

Figure captions

Fig. 1. The SEM images of the synthesized FIOMNs (A), bare SPCE (B), MHAMS@FIOMNs/SPCE (C), and Hb-MHAMS@FIOMNs/SPCE (D). AFM image (E) and XRD pattern (F) of the synthesized FIOMNs.

Fig. 2. (A) Z_p isotherm of FIOMNs by adsorption of different amounts of SDS. (B) Schematic illustration of possible interactions between Hb and MHAMS@FIOMNs for preparation of Hb-MHAMS@FIOMNs biocomposite.

Fig. 3. EIS (A) and cyclic voltammograms (B) of a 0.01 M solution of 1:1 $K_3[Fe(CN)_6]/K_4[Fe(CN)_6]$ with 0.1 M KCl performed on (a) bare SPCE, (b) MHAMS@FIOMNs/SPCE and (c) Hb-MHAMS@FIOMNs/SPCE. (A) Frequency range: 0.1 to 10^5 Hz. (B) Scan rate: 100 mVs^{-1}. Inset: The Randel's equivalent circuit model used to fit the impedance data.

Fig. 4. (A) Cyclic voltammograms of (a) bare SPCE, (b) Hb/SPCE, (c) Hb-MHAMS/SPCE and (d) Hb-MHAMS@ FIOMNs /SPCE in 0.1M PBS pH 7.0 (50 µL) at scan rate of 100 mVs^{-1}. (B) Schematic diagram of the Hb-MHAMS@FIOMNs/SPCE biosensor set-up. (C) part (a): Cyclic voltammograms of Hb-MHAMS@FIOMNs/SPCE in 0.1M PBS pH 7.0 at different scan rates: (1) 20, (2) 50, (3) 100, (4) 150 and (5) 200 mVs^{-1}; part (b): Plot of peak currents vs. scan rate.; part (c): Plot of logarithm of I_{pa} vs. logarithm of υ; and part (d): Plot of peak potentials vs. logarithm of the scan rate (from 0.02 to 1.0 Vs^{-1}).

Fig. 5. (A) Amperometric response of the Hb-MHAMS@FIOMNs/SPCE to successive addition of different concentration of H_2O_2 in 0.1 M PBS (pH 7.0) at the constant potential of −0.43 V. (B) Plot of electrocatalytic peak current vs. H_2O_2 concentration. (C) Plot of the reciprocal of steady-state peak current (I_{ss}) vs. the reciprocal of H_2O_2 concentration for the Hb-MHAMS@FIOMNs/SPCE.

Table 1. Recovery results of H_2O_2 determination using Hb-MHAMS@FIOMNs/SPCE in the commercial mouthwash, rain water, human urine and serum samples (n=3).

Sample	H_2O_2 concentration (μM)		Recovery (%)	RSD (%)
	Spiked	Found		
Mouthwash	-	0.00	-	-
	5.0	4.82	96.4	1.1
	12.0	12.40	103.3	2.5
Urine	-	0.00	-	-
	8.0	7.88	98.5	1.8
	15.0	14.67	97.8	3.1
Serum	-	0.00	-	-
	2.5	2.55	102.00	2.8
	5.0	5.08	101.50	2.2
Rain water	-	0.00	-	-
	10.0	10.10	101.0	2.2
	20.0	19.52	97.6	3.7

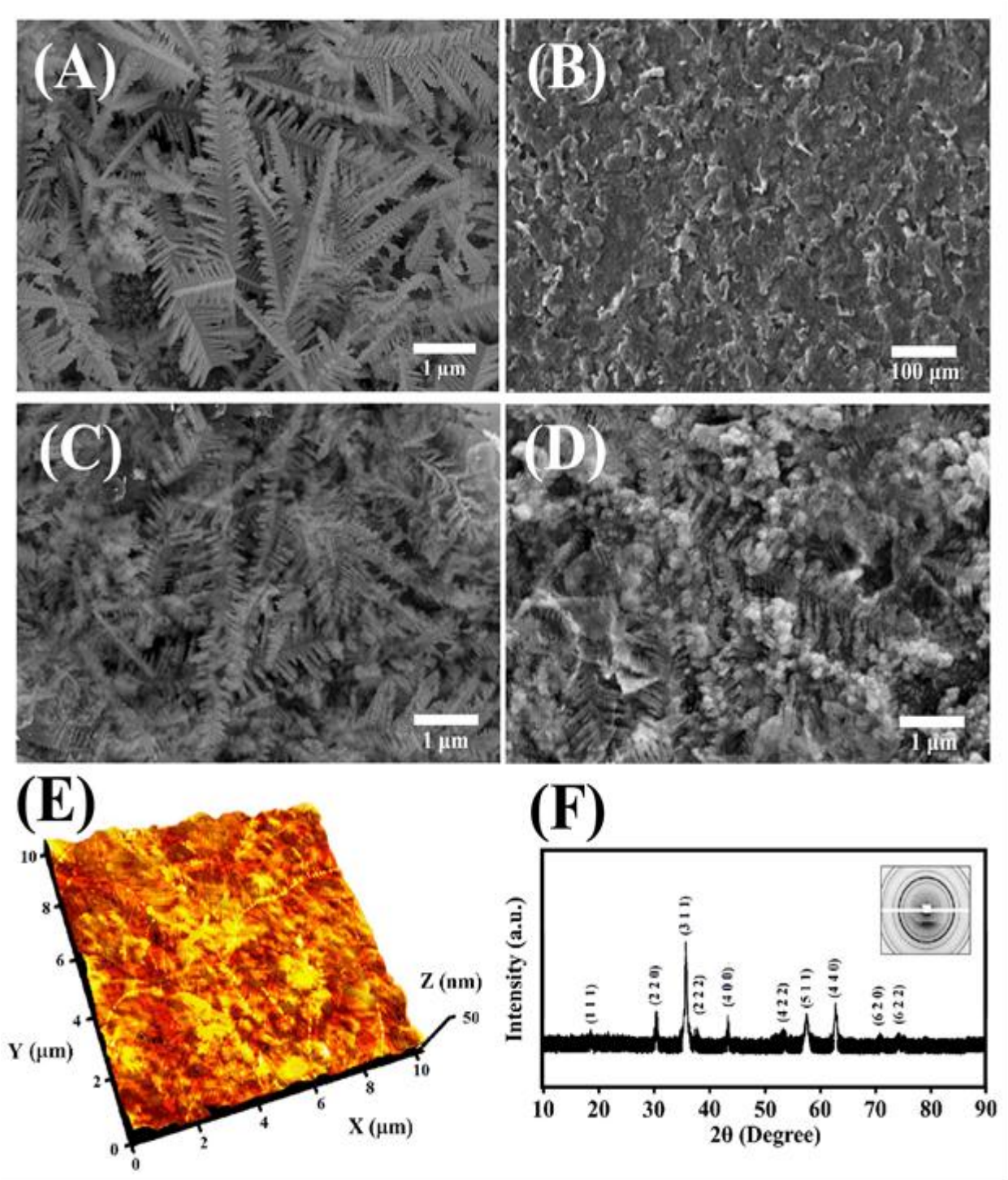
(A)
1 µm
(B)
100 µm
(C)
1 µm
(D)
1 µm
(E)
Y (µm)
X (µm)
Z (nm)
50
(F)
Intensity (a.u.)
(111)
(220)
(311)
(222)
(400)
(422)
(511)
(440)
(620)
(622)
2θ (Degree)

Fig. 1

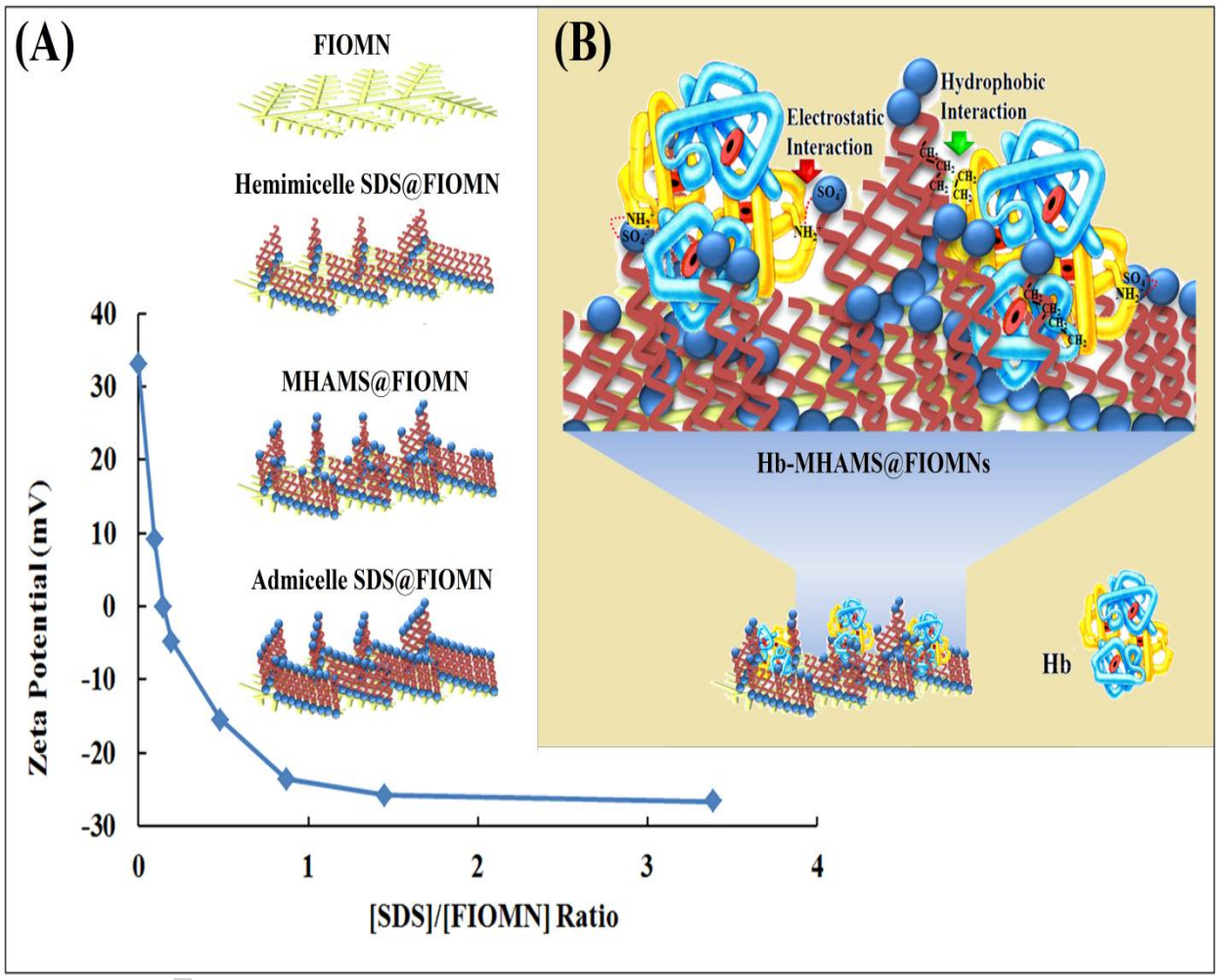
(A)
FIOMN
Hemimicelle SDS@FIOMN
MHAMS@FIOMN
Admicelle SDS@FIOMN
Zeta Potential (mV)
40
30
20
10
0
-10
-20
-30
0
1
2
3
4
[SDS]/[FIOMN] Ratio
(B)
Hydrophobic Interaction
Electrostatic Interaction
Hb-MHAMS@FIOMNs
Hb

Fig. 2

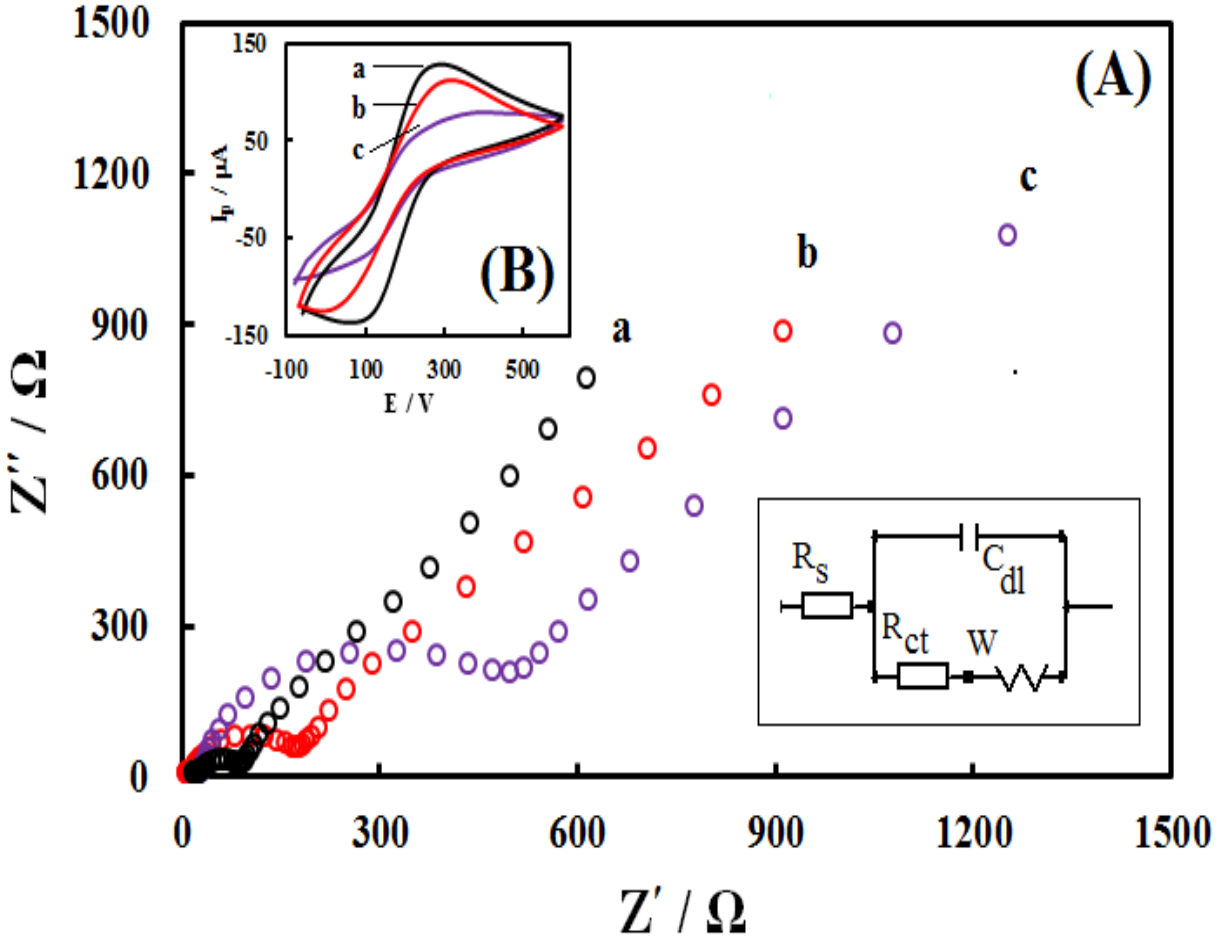

Fig. 3

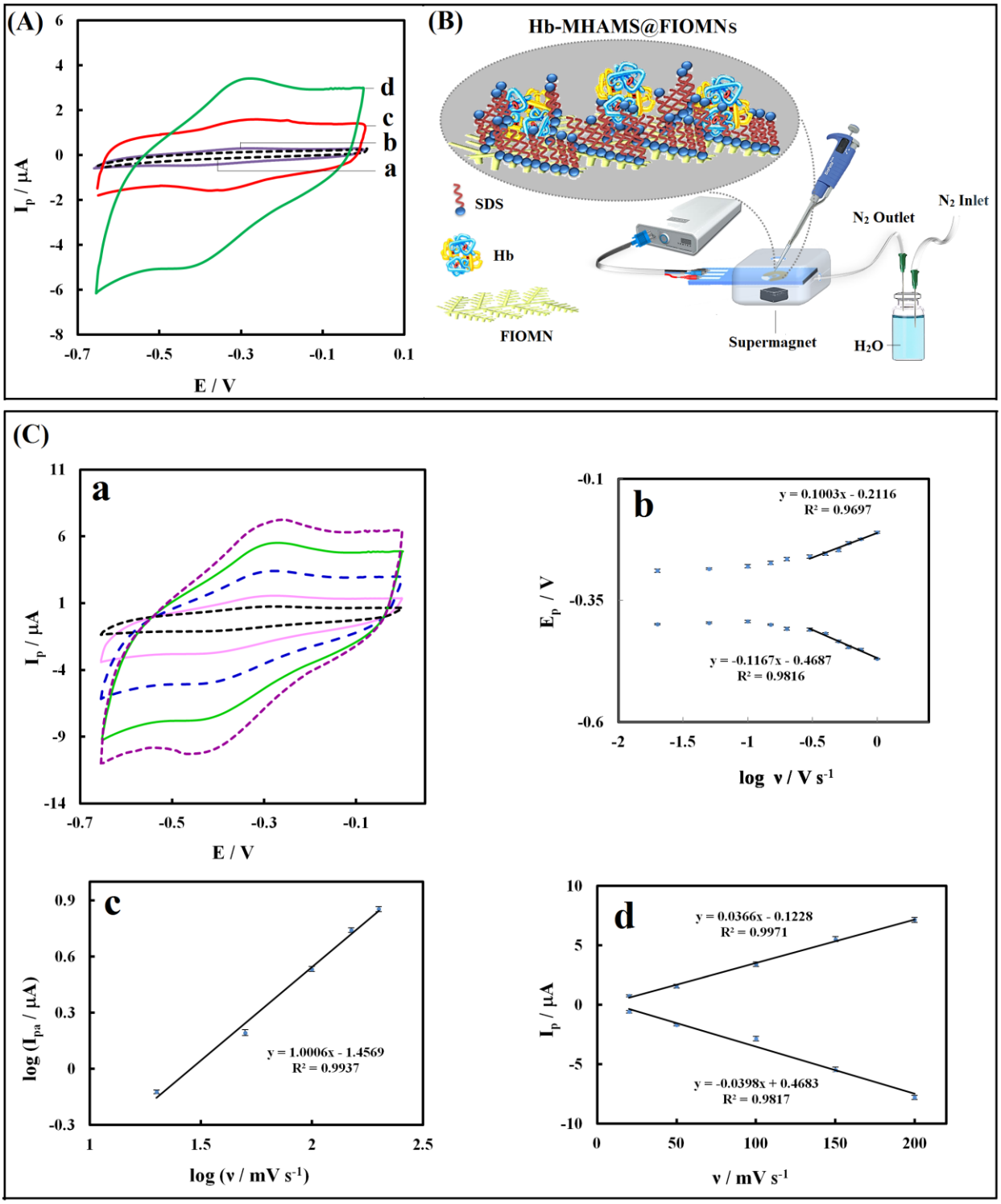
(A)
d
c
b
a
I_p / μA
E / V
(B)
Hb-MHAMS@FIOMNs
SDS
Hb
FIOMN
N_2 Outlet
N_2 Inlet
Supermagnet
H_2O
(C)
a
I_p / μA
E / V
b
y = 0.1003x - 0.2116
R² = 0.9697
y = -0.1167x - 0.4687
R² = 0.9816
E_p / V
log v / V s^{-1}
c
y = 1.0006x - 1.4569
R² = 0.9937
log (I_{pa} / μA)
log (v / mV s^{-1})
d
y = 0.0366x - 0.1228
R² = 0.9971
y = -0.0398x + 0.4683
R² = 0.9817
I_p / μA
v / mV s^{-1}

Fig. 4

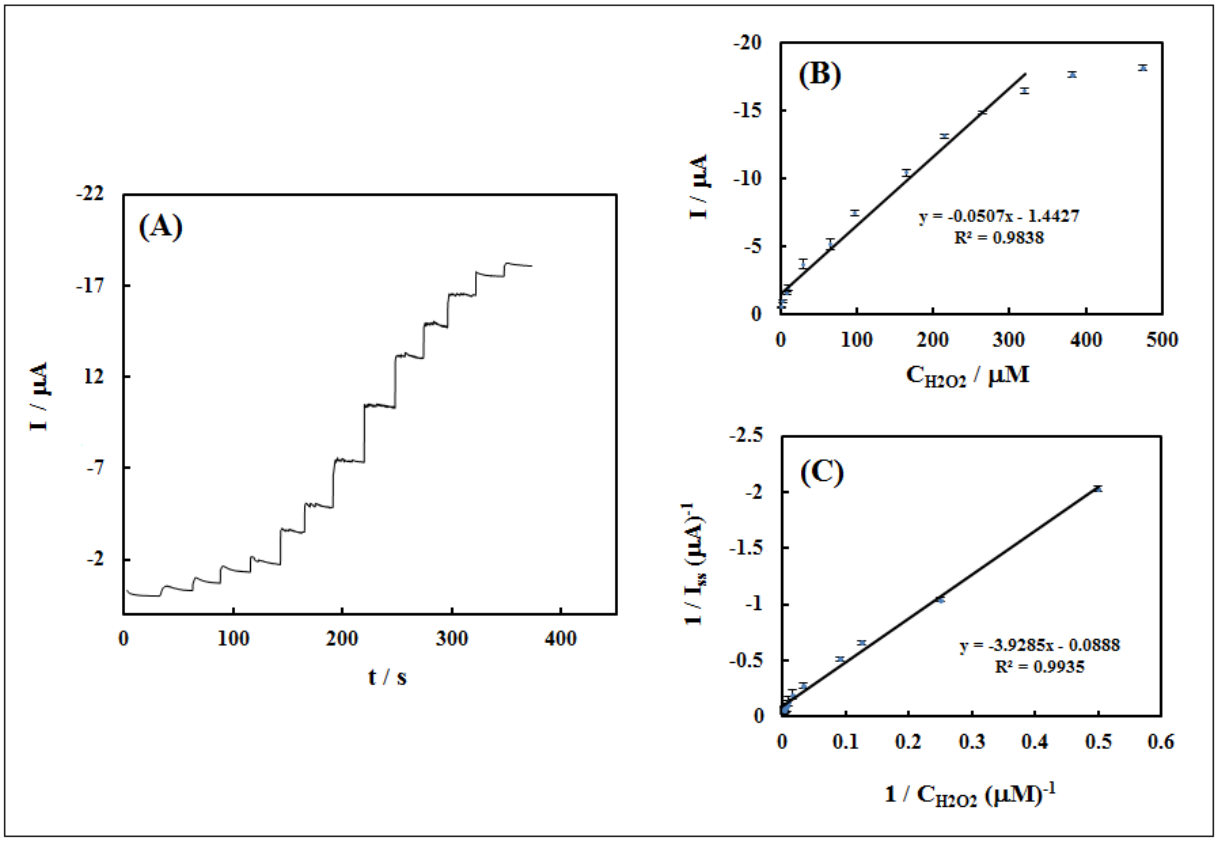

Fig. 5

Research highlights

- Fractal iron oxide magnetic nanostructures uses as a novel host for Hb immobilization
- Gaining mixed hemi/ad-micelle SDS array at FIOMNs by zeta-potential studies
- Facile immobilization of Hb/MHAMS@FIOMNs at SPCE by magnetic force
- Realizing excellent direct electron transfer of Hb at MHAMS@FIOMNs/SPCE
- High analytical performance of biosensortowards H_2O_2 reduction was achieved